

Borderline first-order phase transition and large cryogenic magnetocaloric effect in PrNdIn

Anis Biswas^{*}, Alex Thayer[§], Oleksandr Dolotko[#], Yaroslav Mudryk

Ames National Laboratory, U.S. Department of Energy, Iowa State University, Ames, IA 50011
USA

* Corresponding author: E-mail: anis@ameslab.gov

§ Present address: Blue Origin, LLC, Washington, USA

Present address: Karlsruhe Institute of Technology (KIT), Institute for Applied Materials-
Energy Storage Systems (IAM-ESS), Hermann-von-Helmholtz-Platz 1, D-76344 Eggenstein-
Leopoldshafen, Karlsruhe, Germany

ABSTRACT

We report large cryogenic magnetocaloric effect stemming from an unconventional borderline first-order magnetic phase transition with negligibly small thermomagnetic hysteresis in a rare-earth based intermetallic compound PrNdIn. The sample exhibits maximum magnetic field induced entropy change as large as -10 J/ Kg K (for 20 kOe magnetic field change) near boiling point of oxygen. Magnetocaloric properties of PrNdIn are comparable to those of other known potential magnetocaloric materials with operating temperature ranging between 50 and 125 K. The magnetic properties of present sample are qualitatively reminiscent of those of the binary Pr₂In and Nd₂In, including the emergence of a second low-temperature anomaly in the temperature dependence of magnetization.

I. INTRODUCTION

Magnetic refrigeration (MR) technology is a subject of intense research as one of the better alternatives of currently used gas compression-based refrigeration technology to stymie the ongoing threat of global climate change.¹⁻⁶ The discovery of potential magnetocaloric materials (MCMs) that exhibit large magnetocaloric effects (MCE) suitable for application either near room-temperature or in the cryogenic temperature regime is one of the major challenges for successful practical implementation of MR technology.¹⁻⁸ Initially, paramagnetic salts such as Gadolinium sulphate were used to achieve sub-Kelvin temperatures via cryogenic MCE for which *William E. Giauque* was credited Nobel Prize.⁹ Then, MCE driven refrigeration near room temperature (RT) was conceptually realized¹⁰ using gadolinium metal as an active refrigerant material in several prototype MR devices due to its appreciable large MCE arising from a second order magnetic phase transition (SOMPT) near RT.¹¹ Later, many other transition metal and rare-earth based MCMs, which undergo SOMPTs, have been developed for the application in both ambient and cryogenic temperature ranges.^{7,8,12-16} For cryogenic application, MCMs with operating temperatures near boiling points of different gases such as natural gas, oxygen, and hydrogen are of particular interest considering continuous increase in the consumption of such gases for various renewable energy technologies as well as in the propellant systems of missiles and rockets.^{13,17-19}

The biggest disadvantage of the MCMs showing SOMPT in comparison with those that undergo first-order magnetic phase transition (FOMPT) is their considerably smaller magnetocaloric response especially for the materials targeting near room temperature region. In particular, the discovery of giant MCE in $\text{Gd}_5\text{Si}_2\text{Ge}_2$ ²⁰ led to a huge proliferation of research to design MCMs showing FOMPT.¹⁻⁶ The magnetic transition exhibited by $\text{Gd}_5\text{Si}_2\text{Ge}_2$ is categorized in a special group of FOMPTs known as a first-order magnetostructural transition (FOMST) where a discontinuous magnetic transition between different magnetic states (e.g. from paramagnetic to ferromagnetic) concurrently occurs with changes in both crystallographic bonding and/or lattice symmetry in addition to the changes in lattice parameters.²⁰⁻²² In addition to $\text{Gd}_5(\text{Si}_x\text{Ge}_{1-x})_4$ compounds giant MCE arising due to FOMST is reported in many other material systems, which include transition metal based arsenides²³, Heusler alloys^{24,25}, MnTX (T- transition metals, X- p block elements) type compounds^{26,27}. However, giant MCE is also associated with another type

of FOMPT, termed as first-order magnetoelastic transition (FOMET), for which crystallographic symmetry remains unchanged and bonding is preserved despite a discontinuous change in phase volume and/or lattice parameters occurs conjointly with the magnetic transition.²⁸ Some notable examples of materials showing giant MCE due to FOMET are FeRh^{29,30} and La(Fe_{13-x}Si_x) alloys and their hydrides^{31,32}. It is worth mentioning that the majority of those MCMs exhibiting either FOMST or FOMET are potential candidates for the near room temperature applications while the examples of such materials with FOMPT for cryogenic applications, such as RCo₂ (R=Er, Ho) compounds^{33,34}, are relatively scarce. Recently reported three rare-earth intermetallic R₂In compounds with R= Eu, Pr, and Nd are among those few MCMs showing large MCE in cryogenic temperature range due to FOMET.^{28, 35- 41}

Despite their excellent magnetocaloric responses, there are two major shortcomings of MCMs undergoing FOMPT from the application perspective. The obvious detrimental factor is a thermomagnetic hysteresis, which results in a significant energy loss during temperature and magnetic field cycling of MCM across the transition.^{42,43} Apart from that, the MCMs are often mechanically fragile and deteriorate quickly while undergoing repeated temperature (and/or magnetic field) cycling due to their crystallographic changes across the FOMPT precluding them from been manufactured and used in operating MR devices.^{44,45} Conversely, both thermomagnetic hysteresis and the phase-transition induced mechanical instability of materials are very rare for SOMPTs despite there are a few instances when later is associated with continuous structural transition.^{46,47}

Thus, for practical realization of MR, it is crucial to design potential MCMs with a phase transition where a discontinuous magnetization change, as exhibited by typical FOMPT, coexists with negligible thermomagnetic hysteresis loss and lattice volume change, commonly associated with SOMPT. It is commonly argued that an ideal magnetic phase transition for MCMs would not be either strictly FOMPT or SOMPT, rather it would have characteristic features of both. For example, it has been recently proposed that materials showing the phase transition which lies in between first and second-order would be most suitable for MR.⁶ The foremost research approach to achieve such phase transition, favorable for MR, constitutes chemical and microstructural manipulations of materials showing FOMPT to minimize hysteresis effect and lattice changes across the transition.⁴²

Few materials, mostly transition metal-based, exhibit nearly discontinuous change in magnetization with negligible thermomagnetic hysteresis. In these materials magnetic transition is FOMET arising due to their peculiar itinerant-electron metamagnetic (IEM) character.²⁸ The most notable example is hydrogenated $\text{LaFe}_{13-x}\text{Si}_x$, which exhibits giant MCE near room temperature while the temperature width of thermomagnetic hysteresis corresponding to its first-order transition is just a few Kelvin.³¹ While IEM is uncommon in rare-earth based intermetallics because their magnetism originates from highly localized $4f$ electrons, recently FOMET with negligible thermomagnetic hysteresis was observed for Eu_2In and the first-order nature of the transition retains even with the minor doping of Yb in Eu-site.^{28, 48} Initially these IEM-like transition was believed to be exclusive to Eu_2In due to the divalency of Eu in the compound.^{28,49} However, later it has been experimentally established that similar FOMET with infinitesimally small thermomagnetic hysteresis can occur for other R_2In compounds with R= Pr and Nd where lanthanides are in trivalent states.^{35,39} Remarkably, the crystal structure of R_2In with trivalent R (Ni_2In hexagonal) is different than that of Eu_2In (Co_2Si orthorhombic).^{28,35,39} While the phase transition in Pr_2In is clearly FOMET³⁵, Nd_2In exhibits borderline first-order transition.³⁹ Our detailed density functional theory calculations uncovered that a peculiar feature in the electronic density of states near the Fermi level in both Pr_2In and Nd_2In , strikingly similar to Eu_2In i.e, strong d -character of hybridization between rare-earth d and In- p states near E_F , is likely responsible for their FOMET and it can also be used to explain why borderline first-order transition takes place for Nd_2In .³⁹ Notably, both Pr_2In and Nd_2In exhibit giant cryogenic MCE across their FOMETs around ~ 57 and 110 K, respectively,^{35,39} and that observation raises an important question regarding whether similar phenomenon can occur in case of $(\text{Pr}_{1-x}\text{Nd}_x)_2\text{In}$ solid solution. If mixed $(\text{Pr}_{1-x}\text{Nd}_x)_2\text{In}$ alloys can also show large MCE, then one can easily tune the transition temperature in the range between 57 and 110 K covering boiling points of various technologically important gases such as oxygen, nitrogen, and natural gas. Although both Pr_2In and Nd_2In are isostructural^{35,39}, the site-disorder arising due to the presence of multiple rare-earths in same crystallographic sites, dissimilar crystal field parameters of Nd and Pr⁵⁰, and also their difference in the electronic density of states near Fermi level³⁹ may influence the magnetic transition as well as magnetocaloric properties in case of $(\text{Pr}_{1-x}\text{Nd}_x)_2\text{In}$ compounds, which are yet to be explored.

The main objective of the present work is to address this issue. In this regard, we have carried out extensive experimental study to understand crystallography, magnetic and magnetocaloric properties of PrNdIn.

II. EXPERIMENTAL METHODS

A polycrystalline PrNdIn sample (~ 4 g) was prepared by arc-melting of constituent elements taken in a stoichiometric ratio. The arc-melting was performed in the inert argon atmosphere using Zr as a getter. Among the constituent elements, both Pr and Nd (99.95 wt.% pure with respect to all other elements in the periodic table) were provided by the *Materials Preparation Center of Ames Laboratory*, USA whereas highly pure In (99.995 wt.% pure) was supplied by *Alfa Aesar, USA*. The alloy was re-melted five times, flipping the button upside down after each melt, to achieve best possible mixing of elements so a homogeneous solid solution is formed. The weight loss after melting is less than 0.5% confirming that the ratio of Pr, Nd and In in the prepared alloy is practically identical to the nominal stoichiometric ratio. The arc-melted sample was annealed at 973 K for 3 weeks in a quartz tube sealed under ~0.3 bar high purity helium followed by slow cooling down inside the furnace after the latter was turned off at the end of the annealing process. The same heat treatment procedure was followed to prepare Nd₂In and Pr₂In in our previous studies.^{35,39} Considering possible reactivity with air known to occur in many R₂In alloys^{28,35,39}, the prepared PrNdIn sample was stored and handled inside an Ar-filled glovebox, where oxygen and moisture levels were maintained below 1 ppm.

To verify crystal structure of the prepared alloy, powder x-ray diffraction (PXR) study was performed by employing a Philips X'Pert Pro diffractometer equipped with Cu-K_α radiation. For this purpose, sample powder was prepared by grinding with agate pestle in the agate mortar and then it was mounted on a Si sample holder inside the glove box. The sample holder with powder was covered with Kapton film inside the glove box to prevent powder exposure to the air during the PXR scan. The Rietveld refinement of PXR data was performed using FullProf.⁵¹

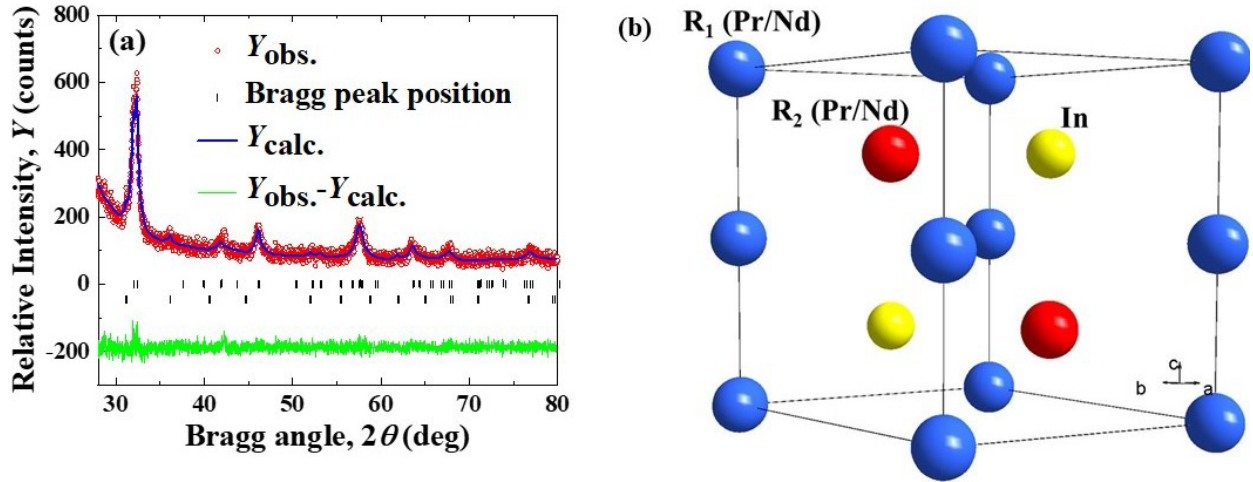


FIG. 1. (a) Rietveld refinement of the powder X-ray diffraction pattern of the PrNdIn sample recorded at room temperature. (b) Schematic representation of the Ni_2In -type prototypical crystal structure (space group $P6_3/mmc$): the rare-earth atoms (Pr and Nd) occupy two symmetrically distinct sites designated as R_1 (blue spheres) and R_2 (red spheres) while yellow spheres indicates the position of In in this hexagonal unit cell.

The magnetic properties of the sample were studied using a Superconducting Quantum Interference Device (SQUID) magnetometer, MPMS XL-7 (Quantum Design Inc.). To assess the magnetic transition as well as the thermomagnetic hysteresis, the temperature dependencies of dc magnetization, $M(T)$, were studied in the temperature range from 5 to 175 K in the presence of 2 kOe and 20 kOe applied magnetic fields. The sample was cooled down to 5 K in the presence of a desired magnetic field before every measurement and then $M(T)$ was recorded during the warming and cooling cycles in that constant magnetic field to investigate thermomagnetic hysteresis. The temperature ramping rate during measurement is 0.5 K per minute. The magnetic transition temperature, T_C , was defined as the temperature corresponding to the minimum of $\partial M(T)/\partial T$ for a given H where the fastest change in $M(T)$ was manifested. The magnetic field-induced entropy change (ΔS), an important magnetocaloric parameter, was calculated from $M(T)$ data recorded for different H during warming cycle using Maxwell's relation.⁵²

To get an idea about magnetic ground state, magnetic field dependence of magnetization, $M(H)$, was studied at 5 K for the magnetic fields ranging from -50 to 50 kOe and also the first quadrant of $M(H)$ curve was measured between 0 and 120 kOe magnetic field using the vibrating

sample magnetometer of the physical properties measurement system PPMS-VSM (Quantum Design Inc.).

The phase transition was further verified by specific heat (C_p) measurement using a conventional relaxation method in the temperature range from 2 to 100 K on the same PPMS setup.

III. EXPERIMENTAL RESULTS AND DISCUSSIONS

Phase analysis of the collected PXRD pattern (Fig. 1a) confirms formation of the Ni_2In type hexagonal (space group $P6_3/mmc$) phase as a majority phase ($\sim 90\%$) together with a secondary R_3In -type impurity phase ($\sim 10\%$), which is reminiscent to the cases of Pr_2In ³⁵ and Nd_2In ³⁹. As shown in Fig. 1b, in this Ni_2In type hexagonal structure, rare-earth atoms (Nd and Pr) occupy two symmetry-distinctive crystallographic sites in $2a$ ($x = y = z = 0$) and in $2d$ ($x = 1/3, y = 2/3, z = 3/4$), while In atoms are located in $2c$ with $x = 1/3, y = 2/3, z = 1/4$. The Rietveld analysis reveals that the lattice parameters for the hexagonal unit cell for the sample are: $a = b = 5.5257$ (12) Å, $c = 6.8921$ (15) Å with unit cell volume, $V = 182.24$ (7) Å³, which is in between of Pr_2In ³⁵ and Nd_2In ³⁹. The lattice parameter of the secondary (Pr,Nd)₃In phase with cubic lattice symmetry is $a = 4.971(1)$ Å.

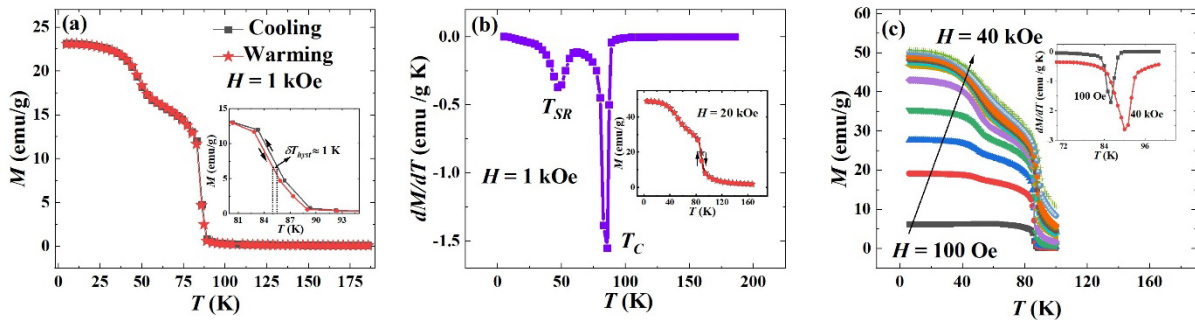


FIG. 2. (a) Temperature dependence of magnetization in applied magnetic field of 1 kOe recorded during both cooling (black-colored symbols) and warming (red-colored symbols) cycles. Inset: Expanded view of $M(T)$ curve in the temperature range near transition at $T_C \sim 86$ K showing negligible thermomagnetic hysteresis between cooling and heating curve. (b) dM/dT vs. T curve derived from $M(T)$ for $H = 1$ kOe during warming cycle clearly shows minimums both at T_C and at T_{SR} . Inset: $M(T)$ curve recorded during warming and cooling at $H = 20$ kOe. (c) $M(T)$

curves recorded in FCW protocol for different applied magnetic fields of 100 Oe, 500 Oe, 1 kOe, 2 kOe, 5 kOe, 10 kOe, 12.5 kOe, 15 kOe, 17.5 kOe, 20 kOe, 30 kOe, and 40 kOe. Inset: comparison of dM/dT vs. T curves for $H= 100$ Oe and 40 kOe, which clearly reveals there is slight but noticeable increase of T_C with the increase of applied magnetic fields.

The $M(T)$ data for PrNdIn (Fig. 2a,b) also appears to be qualitatively similar to that observed for $\text{Pr}_2\text{In}^{35}$ and $\text{Nd}_2\text{In}^{39}$ i.e, a sharp paramagnetic to ferromagnetic transition followed by an anomaly at lower temperature. For the present sample, T_C is at ~ 86 K (Fig. 2b), which is very close to the temperature corresponding to the mean of T_C s of $\text{Pr}_2\text{In}^{35}$ and $\text{Nd}_2\text{In}^{39}$ in agreement with the de Gennes scaling relation for the transition temperatures in rare-earth based compounds.^{53,54} The sharpness of that transition is an indication of the FOMPT and there is no detectable thermomagnetic hysteresis between cooling and warming $M(T)$ curves at the transition (Fig. 2a and inset of Fig. 2b), which also replicates thermomagnetic behavior of $\text{Nd}_2\text{In}^{39}$ and $\text{Pr}_2\text{In}^{35}$. The second magnetic anomaly is observed around $T_{\text{SR}} \sim 50$ K, which is likely due to a spin-reorientation transition present in binary R_2In ($\text{R} = \text{Pr}$ and Nd) compounds as well.^{35,39} However, a true nature of this spin-reorientation transition cannot be revealed through magnetic measurement of polycrystalline sample. Therefore, neutron diffraction experiment is required to probe the magnetic structure of both binary and pseudobinary R_2In compounds and it is planned as a follow-up study. The application of higher magnetic fields broadens the transition and shifts the T_C slightly ($dT_C/dH \sim 0.01$ K (kOe)⁻¹), whereas the T_{SR} remains unchanged (Fig. 2c). The effective paramagnetic moment of the sample (μ_{eff}), determined from linear H/M versus T curve above T_C according to Curie-Weiss law is $\sim 5.11 \mu_{\text{B}}/\text{f.u}$ and Weiss temperature, θ_p is ~ 70 K. If we consider Pr and Nd are homogeneously distributed with equal occupancy in the $2a$ and $2d$ crystallographic sites of the hexagonal crystal structure, the theoretically calculated μ_{eff} would be $\sim 5.09 \mu_{\text{B}}/\text{f.u}$, which is very close to its experimentally obtained value ($\sim 5.11 \mu_{\text{B}}/\text{f.u}$).

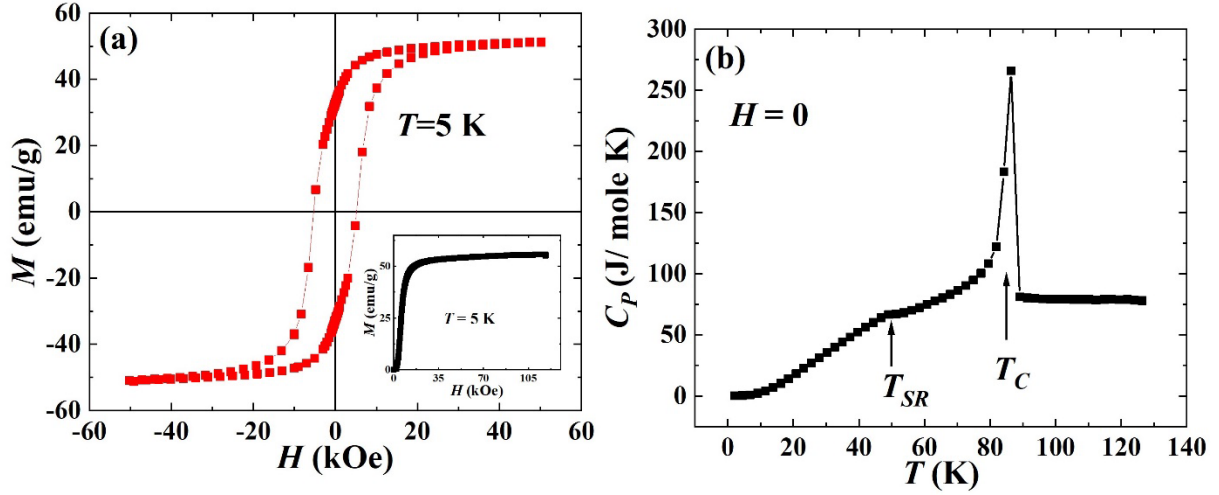


FIG. 3. (a) PrNdIn $M(H)$ hysteresis loop recorded in magnetic field ranging between +50 kOe and -50 kOe. Inset: the first-quadrant $M(H)$ curve measured between 0 and 120 kOe. (b) The temperature dependence of heat capacity, C_p , recorded in the absence of applied magnetic field. The transitions at T_C and T_{SR} are clearly manifested through sharp peak and broad hump in the curve, respectively.

The $M(H)$ curve recorded at 5 K between -50 and $+50$ kOe shows typical ferromagnetic hysteresis loop with coercivity $H_C \sim 5$ kOe (Fig. 3a). The presence of H_C is an indication of the presence of magnetocrystalline anisotropy in the sample. In this regard, one can recall that Pr_2In exhibits even larger H_C ³⁵ whereas for Nd_2In H_C is a few hundred Oe³⁹. Thus it can be inferred that magnetocrystalline anisotropy likely decreases with the increase of $x(\text{Nd})$ in the $(\text{Pr}_{1-x}\text{Nd}_x)_2\text{In}$ system. We determine saturation magnetization, M_S , using the $M(H)$ data recorded up to 120 kOe (inset to Fig. 3a). The experimentally obtained $M_S = 3.94 \mu_B/\text{f.u.}$ is considerably lower than theoretical $gJ = 6.47 \mu_B/\text{f.u.}$ Even considering that only 90% of the sample belongs to the main phase and the actual M_S may be slightly higher, there is an obvious magnetic moment reduction in PrNdIn. The similar behavior of saturation magnetization is also observed for both Pr_2In and Nd_2In .^{35,39,55} It has been already experimentally established that strong crystalline electric field (CEF) effect is present in the majority of the R_2In type compounds except $\text{R} = \text{Gd}$,⁵⁰ and it likely leads to the splitting of the energy levels of $4f$ manifold and the reduction of R^{3+} moments.^{35,39} The possibility of non-collinear magnetic structure instead of the collinear ferromagnetic nature of magnetic ground state in such compounds cannot be ruled out to explain lower than observed magnetic moment. However, the lack of moment rotation signatures in the

$M(H)$ data up to 120 kOe does not support this hypothesis. One can also consider that the RKKY-type exchange interactions can be ferromagnetic and antiferromagnetic depending on the distance and the electron density near Fermi level (E_F) between the rare-earth atoms. In the present case, Pr^{3+} and Nd^{3+} are randomly distributed in the crystal lattice and, depending on how much their dissimilarities affect the electron density near E_F , the magnetic interactions could vary when compared with the binary compounds. Therefore, overall magnetic moment can also vary from theoretical value as later is calculated by assuming simple ferromagnetic state with no perturbations from the lattice environment. Further, the ground state of material may be ferrimagnetic, which would also consistent with the $M(T)$ and $M(H)$ curves that we have obtained.

The magnetic transitions are further confirmed by heat capacity measurement, $C_p(T)$, through the manifestation of a sharp peak around T_C along with a broad one at T_{SR} , Fig. 3b. While the peak around T_C is quite sharp, it is also highly asymmetric - nearly λ -shaped - contrary to the appearance of a typical δ -shaped peak associated with FOMPT, e.g. in Pr_2In .³⁵ At the same time, one should consider the fact that the theoretically infinite heat capacity associated with FOMPT often is not clearly resolved within typical temperature resolution of the standard 2τ analysis of the raw heat capacity data obtained using a relaxation method of C_p measurement in PPMS.²⁸ Further, if the transition is borderline between first and second order, e.g. in Nd_2In , similar sharp asymmetric peak can also arise in $C_p(T)$ as well.³⁹

The sharp magnetic transition at T_C in the sample warrants probing it for large MCE. In addition, the analysis of magnetocaloric parameter, ΔS , can unambiguously resolve the doubt regarding the nature of the phase transition as well.⁵⁶ Hence we studied the magnetocaloric properties of PrNdIn . The temperature dependence of $-\Delta S$ determined from the $M(T)$ data for different fields up to 40 kOe (Fig. 4a) indeed indicates quite large value of ΔS_{Max} around $T_C \sim 87$ K, which is close to the boiling point of oxygen. The obtained $\Delta S_{Max} = -10$ J/ Kg K for $\Delta H = 20$ kOe (-13.5 J/ Kg K for $\Delta H = 40$ kOe) in case of present PrNdIn sample is less compared to that observed for both Pr_2In ³⁵ and Nd_2In ³⁹ due to its slightly broader transition in comparison with the latter two. However, the value is comparable to other potential rare-earth intermetallic MCMs in the operating temperature range of 50 to 125 K and is considerably larger than that of other R_2In type compounds showing SOMPT (Fig. 4b).^{13,17, 28,33,34, 35,39, 57 - 63} We calculated relative cooling

power (*RCP*) and refrigerant capacity (*RC*) of this material from $-\Delta S(T)$ for $\Delta H = 20$ kOe.³ The obtained values of *RC* and *RCP* are 27 J/Kg and 39 J/Kg, which are comparable with those calculated from $-\Delta S(T)$ for Nd_2In ³⁹ whereas those are less than Pr_2In ³⁶. We also observed that while Pr_2In is extremely air sensitive and decomposed in ambient condition, the doping of Nd in Pr site, enhances the stability of the alloys in ambient condition which is important from the application point of view. In addition to the composition of our present sample, which is exactly at the middle of the solid solution $(\text{Pr}_{1-x}\text{Nd}_x)_2\text{In}$, it is likely to observe appreciably large MCEs for other members of the series with $0 < x < 1$ in the temperature range between 57 K and 110 K. Apart from the peak at T_C , a second broad maximum is also observed for PrNdIn in $-\Delta S(T)$ around T_{SR} .

To identify whether the transition is first- or second-order in nature, we carefully examine the universal behavior of $-\Delta S(T)$ obtained at different ΔH following the analysis of *Bonilla et al.*⁶⁴ According to their study, all $-\Delta S(T)$ curves (normalized to peak value) for different ΔH in case of a second-order ferromagnetic (and ferrimagnetic) transition must collapse onto a universal curve when the temperature axis is rescaled as follows:⁶⁴

$$\theta = -\frac{(T-T_C)}{(T_{r1}-T_C)} \text{ for } T \leq T_C, \text{ and,}$$

$$\theta = \frac{(T-T_C)}{(T_{r2}-T_C)} \text{ for } T > T_C \quad \dots\dots\dots(2)$$

Where T_{r1} and T_{r2} are reference temperatures, respectively, below and above T_C that satisfy the relation $\Delta S(T_{r1})/\Delta S_{\text{Max}} = \Delta S(T_{r2})/\Delta S_{\text{Max}} = h$

On the other hand, such universal behavior would not hold for a typical FOMPT.⁶⁴ As shown in Fig. 4c, a universal curve cannot be successfully constructed for PrNdIn and there is

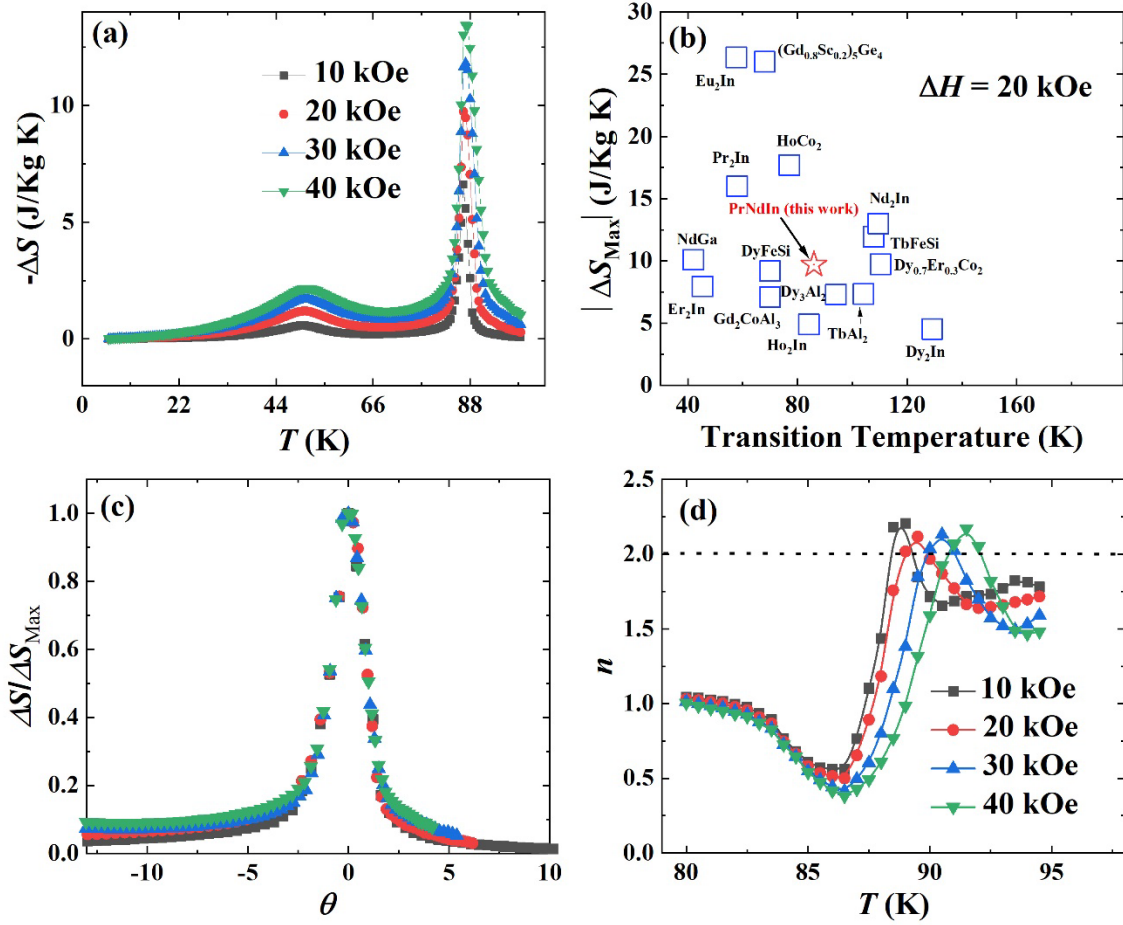


FIG. 4. (a) The temperature dependence of ΔS for $\Delta H = 10, 20, 30,$ and 40 kOe exhibited by present PrNdIn. (b) Comparison of the maximum value of ΔS , ΔS_{Max} obtained for PrNdIn for $\Delta H = 20$ kOe with other known potential magnetocaloric materials in operating temperature range: $40-120$ K as well as other R_2In compounds [Ref.(s): 13,17, 28,33,34, 35,39, 65- 71]. (c) The construction of universal curve taking into account $-\Delta S(T)$ curves recorded for $\Delta H = 10, 20, 30,$ and 40 kOe. (d) The temperature dependence on n , calculated from $-\Delta S(\Delta H, T)$ according to equation 4.

a significant discrepancy between the curves below $\theta = -1$, a typical feature of materials showing FOMPT.⁶⁴ We quantified the goodness of the collapsing of every scaled curves into the single universal curve by defining dispersion (d) as follows:^{64, 72}

$$d(\theta) = 100 \times \frac{W(\theta)}{\Delta S / \Delta S_{Max}(\theta)} \dots\dots\dots(3)$$

Here, W is the width of vertical spreading of scaled curves for a given θ . For the present sample, d is $\sim 75\%$ for all points of universal curve below $\theta = -1$. Earlier studies point out that d can never exceed 30% for SOMPT.^{64,73} While d for present sample is larger than accepted for SOMPT ruling out possibility of second-order nature of transition, it is also smaller than that obtained for materials showing typical FOMPT as for the latter $d > 100\%$ below $\theta = -1$.⁶⁴ From this, it can be inferred that magnetic transition at T_C for PrNdIn is a boarder-line first-to-second order transition.

The thermodynamic nature of the phase transition can also be precisely determined from the magnetic field dependence of ΔS .⁵⁶ Generally ΔS can be expressed as:^{56,72,73}

$\Delta S \propto H^n$ where the exponent, n is both H and T dependent as:

$$n(H, T) = \frac{d \ln|\Delta S|}{d \ln(H)} \dots\dots\dots(4)$$

It has been demonstrated that $n(H, T)$ profile determined using equation (4) for materials showing typical FOMPT must show a maximum with $n \gg 2$ near the transition temperature. As shown in Fig. 4d, a clear maximum is evident for $n(H, T)$ for all magnetic fields in case of present sample near its T_C while the maximum value of n is almost equal to or slightly larger than 2. This $n(H, T)$ feature further proves that magnetic transition at T_C for PrNdIn is of thr first-order nature according to previous study by *Law et al.*⁵⁶ However, considering the maximum value of n barely exceeding over 2, one can also assume that transition is just a borderline case of FOMPT as observed in the case of Nd₂In³⁹. Further, we acknowledge that the analysis by *Law et al.*⁵⁶ was strictly valid for the single-phase materials while our sample contains secondary phase (R₃In-type) of approximately 10%. Since the magnetic transition temperature of impurity phase would not coincide with T_C and there is no additional anomaly in $M(T)$, other than two characteristic transitions associated with majority R₂In-type phase, the model developed by *Law et al.*⁵⁶ would be valid for this case. Nevertheless, we believe that the main conclusions of this work, in particular the borderline nature of the phase transition, are not substantially affected by the presence of impurity. Considering previously obtained results on Pr₂In and Nd₂In compounds^{35,39} such borderline FOMPT is likely associated with a very small change of crystallographic

parameters and cell volume during the transition and hence the thermomagnetic hysteresis at T_C is negligibly small.

IV. SUMMARY

We experimentally demonstrate the occurrence of a borderline first-order transition with infinitesimally small thermomagnetic hysteresis for PrNdIn at $T_C = 86$ K, close to boiling point of oxygen. The obtained $-\Delta S_{Max} = 10$ J/ Kg K for the $\Delta H = 20$ kOe is comparable to other known potential magnetocaloric materials for cryogenic application in the temperature range between 50 and 125 K. The T_C of PrNdIn is in the middle between the T_C 's of Pr₂In and Nd₂In. The qualitative similarity of magnetic behavior of PrNdIn with Pr₂In and Nd₂In including a second low temperature anomaly in $M(T)$ endorses the fact that the sharp magnetic transition along with large MCE is likely achievable in all compositions belonging to the solid solution of (Pr_{1-x}Nd_x)₂In and that enables tuning of the transition temperature in a wider range between 57 K (T_C of Pr₂In) and 110 K (T_C of Nd₂In) covering boiling points of different technologically important gases including oxygen, nitrogen, and natural gas.

ACKNOWLEDGEMENTS

Authors would like to pay gratitude to late Prof. Vitalij K. Pecharsky, who was initially involved with this work. This work was performed at Ames National Laboratory and supported by the Division of Materials Science and Engineering of the Office of Basic Energy Sciences, Office of Science of the U.S. Department of Energy (DOE). Ames Laboratory is operated for the U.S. DOE by Iowa State University of Science and Technology under Contract No. DE-AC02-07CH11358.

DATA AVAILABILITY

The data that support the findings of this study are available from the corresponding author upon reasonable request.

¹ E. Brück, “Developments in magnetocaloric refrigeration”, Journal of Physics D: Applied Physics **38**, R381 (2005).

-
- ² V. K. Pecharsky, and K. A. Gschneidner, Jr., “Magnetocaloric effect and magnetic refrigeration”, *Journal of Magnetism and Magnetic Materials* **200**, 44 (1999).
- ³ K. A. Gschneidner, Jr., and V. K. Pecharsky, “Magnetocaloric Materials”, *Annual Review of Materials Science* **30**, 387 (2000).
- ⁴ A. Kitanovski, “Energy Applications of Magnetocaloric Materials”, *Advanced Energy Materials* **10**, 1903741 (2020).
- ⁵ X. Moya, and N. D. Mathur, “Caloric materials for cooling and heating”, *Science* **370**, 797 (2020).
- ⁶ V. Franco, J. S. Blázquez, J. J. Ipus, J. Y. Law, L. M. Moreno-Ramírez, and A. Conde, “Magnetocaloric effect: From materials research to refrigeration devices”, *Progress in Materials Science* **93**, 112 (2018).
- ⁷ Y. Mudryk, and V. K. Pecharsky, “Materials for Solid State Cooling” in *Rare Earth Chemistry* Ed. By R. Pottgen, T. Justel, C. A. Strassert, and De Gruyter, Pg. 487 (2020).
- ⁸ J. Y. Law, L. M. Moreno-Ramirez, A. Diaz-Garcia, and V. Franco, “Current perspective in magnetocaloric materials research”, *Journal of Applied Physics* **133**, 040903 (2023)
- ⁹ W. F. Giaque, and D. P. MacDougall, “Attainment of Temperatures Below 1° Absolute by Demagnetization of $Gd_2(SO_4)_3 \cdot H_2O$ ” *Physical Review* **43**, 768 (1933).
- ¹⁰ G. V. Brown, “Magnetic heat pumping near room temperature”, *Journal of Applied Physics* **47**, 3673 (1975).
- ¹¹ A. Kitanovski, J. Tusek, U. Tomc, M. Ozbolt, and A. Poredos, “Overview of Existing Magnetocaloric Prototype Devices” In: *Magnetocaloric Energy Conversion. From Theory to Application*, Springer, Pg. 269 (2015).
- ¹² K. A. Gschneidner, Jr., V. K. Pecharsky, and A. O. Tsokol, “Recent developments in magnetocaloric materials”, *Reports on Progress in Physics* **68**, 1479 (2005).

-
- ¹³ H. Zhang, Y. J. Sun, E. Niu, L. H. Yang, J. Shen, F. X. Hu, J. R. Sun, and B. G. Shen, “Large magnetocaloric effects of RFeSi ($R = \text{Tb}$ and Dy) compounds for magnetic refrigeration in nitrogen and natural gas liquefaction”, *Applied Physics Letters* **103**, 202412 (2013).
- ¹⁴ P. O. Ribeiro, B. P. Alho, R. S. De Oliveira, E. P. Nobrega, V. S. R. de Sousa, P. J. von Ranke, A. Biswas, M. Khan, Y. Mudryk, and V. K. Pecharsky, “Magnetothermal properties of $\text{Ho}_{1-x}\text{Dy}_x\text{Al}_2$ ($x = 0, 0.05, 0.10, 0.15, 0.25$ and 0.50) compounds”, *Journal of Magnetism and Magnetic Materials* **544**, 168705 (2022).
- ¹⁵ A. Biswas, T. Del Rose, Y. Mudryk, P. O. Ribeiri, B. P. Alho, V. S. R. de Sousa, E. P. Nóbrega, P. j. von Ranke, and V. K. Pecharsky, “Hidden first-order phase transitions and large magnetocaloric effects in $\text{GdNi}_{1-x}\text{Co}_x$ ”, *Journal of Alloys and Compounds* **897**, 163186 (2022).
- ¹⁶ B. P. Alho, P. O. Ribeiro, V. S. R. de Sousa, B. C. Margato, A. Biswas, T. Del Rose, R. S. de Oliveira, E. P. Nobrega, P. J. von Ranke, Y. Mudryk, V. K. Pecharsky, “Fathoming the anisotropic magnetoelasticity and magnetocaloric effect in GdNi ”, *Physical Review B* **106**, 184403 (2022)
- ¹⁷ F. W. Wang, X. X. Zhang, and F. X. Hu, “Large magnetic entropy change in TbAl_2 and $(\text{Tb}_{0.4}\text{Gd}_{0.6})\text{Al}_2$ ”, *Applied Physics Letters* **77**, 1360 (2000).
- ¹⁸ See <https://igu.org/resources/global-gas-report-2020/> for “Global Gas Report” (2020).
- ¹⁹ W. Liu, T. Gottschall, F. Scheibel, E. Bykov, N. Fortunato, A. Aubert, H. Zhang, K. P. Skokov, and O. Gutfleisch, “Designing magnetocaloric materials for hydrogen liquefaction with light rare-earth laves phases”, *Journal of Physics :Energy*, DOI 10.1088/2515-7655/accb0b
- ²⁰ V. K. Pecharsky, and K. A. Gschneidner, Jr., “Giant Magnetocaloric Effect in $\text{Gd}_5(\text{Si}_2\text{Ge}_2)$ ”, *Physical Review Letters* **78**, 4494 (1997).
- ²¹ L. Morellon, P. A. Algarabel, M. R. Ibarra, J. Blasco, B. Garcia-Landa, Z. Arnold, F. Albertini, “Magnetic-field-induced structural phase transition in $\text{Gd}_5(\text{Si}_{1.8}\text{Ge}_{2.2})$ ”, *Physical Review B* **58**, R14721 (1998).

-
- ²² S. B. Roy, “First-order magneto-structural phase transition and associated multi-functional properties in magnetic solids”, *Journal of Physics: Condensed Matter* **25**, 183201 (2013).
- ²³ G. A. Govor, V. I. Mitsiuk, S. A. Nikitin, N. Yu. Pankratov, and A. I. Smarzhevskaya “Magnetostructural phase transitions and magnetocaloric effect in Mn(As,P) compounds and their composites”, *Journal of Alloys and Compounds* **801**, 428 (2019).
- ²⁴ T. Krenze, E. Duman, M. Acet, E. Wassermann, X. Moya, L. Manosa, and A. Planes, “Inverse magnetocaloric effect in ferromagnetic Ni-Mn-Sn alloys”, *Nature Materials* **4**, 450 (2005).
- ²⁵ H. N. Bez, A. K. Pathak, A. Biswas, N. Zarkevich, V. Balema, Y. Mudryk, D. D. Johnson, and V. K. Pecharsky, “Giant enhancement of the magnetocaloric response in Ni–Co–Mn–Ti by rapid solidification”, *Acta Materialia* **173**, 225 (2019).
- ²⁶ A. Biswas, A. K. Pathak, N. A. Zarkovich, X. Liu, Y. Mudryk, V. Balema, D. D. Johnson, and V. K. Pecharsky, “Designed materials with the giant magnetocaloric effect near room temperature”, *Acta Materialia* **180**, 341 (2019).
- ²⁷ A. Biswas, N. A. Zarkevich, Y. Mudryk, A. K. Pathak, A.V. Smirnov, V. P. Balema, D. D. Johnson, and V. K. Pecharsky, “Controlling magnetostructural transition and magnetocaloric effect in multi-component transition-metal-based materials”, *Journal of Applied Physics*. **129**, 193901 (2021).
- ²⁸ F. Guillou, A. K. Pathak, D. Paudyal, Y. Mudryk, F. Wilhelm, A. Rogalev, and V. K. Pecharsky, “Non-hysteretic first-order phase transition with large latent heat and giant low-field magnetocaloric effect”, *Nature Communications* **9**, 2925 (2018).
- ²⁹ L. H. Lewis, C. H. Marrows, and S. Langridge, “Coupled magnetic, structural, and electronic phase transitions in FeRh”, *Journal of Physics D: Applied Physics* **49**, 323002 (2016).
- ³⁰ A. Biswas, S. Gupta, D. Clifford, Y. Mudryk, R. hadimani, R. Barua, and V. K. Pecharsky, “Bulk-like First-Order Magnetoelastic Transition in FeRh particles”, *Journal of Alloys and Compounds* **921**, 165993 (2022).

-
- ³¹ A. Fujita, S. Fujieda, Y. Hasegawa, and K. Fukamichi, “Itinerant-electron metamagnetic transition and large magnetocaloric effects in $\text{La}(\text{Fe}_x\text{Si}_{1-x})_{13}$ compounds and their hydrides”, *Physical Review B* **67**, 104416 (2003).
- ³² L. F. Bao, F. X. Hu, L. Chen, J. Wang, J. R. Sun, and B. G. Shen, “Magnetocaloric properties of $\text{La}(\text{Fe},\text{Si})_{13}$ - based material and its hydride prepared by industrial mischmetal, *Applied Physics Letters* **101**, 162406 (2012)
- ³³ H. Wada, S. Tomekawa, M. Shiga, “Magnetocaloric properties of a first-order magnetic transition system ErCo_2 ”, *Cryogenics* **39**, 915 (1999)
- ³⁴ V. Sechovsky, D. Vasylyev, and J. Prokleska, “Magnetocaloric and Thermal Properties of $\text{Ho}(\text{Co}_{1-x}\text{Si}_x)_2$ Compounds”, *Zeitschrift für Naturforschung* **62b**, 965 (2007)
- ³⁵ A. Biswas, N. A. Zarkevich, A. K. Pathak, O. Dolotko, I. Z. Hlova, A. V. Smirnov, Y. Mudryk, D. D. Johnson, and V. K. Pecharsky, “First-order magnetic phase transition in Pr_2In with negligible thermomagnetic hysteresis”, *Physical Review B* **101**, 224402 (2020).
- ³⁶ A. Biswas, R. K. Chouhan, O. Dolotko, A. Thayer, S. Lapidus, Y. Mudryk, and V. K. Pecharsky, “Correlating crystallography, magnetism, and electronic structure across an hysteretic first-order phase transition in Pr_2In ”, *ECS Journal of Solid State Science and Technology* **11**, 043005 (2022).
- ³⁷ B. P. Alho, P. O. Ribeiro, P. J. von Ranke, F. Guillou, Y. Mudryk, and V. K. Pecharsky, “Free-energy analysis of the nonhysteretic first-order phase transition of Eu_2In ”, *Physical Review B* **102**, 134425 (2020).
- ³⁸ D. H. Ryan, D. Paudyal, F. Guillou, Y. Mudryk, A. K. Pathak, and V. K. Pecharsky, “The first-order magnetoelastic transition in Eu_2In : A ^{151}Eu Mössbauer study”, *AIP Advances* **9**, 125137 (2019).
- ³⁹ A. Biswas, R. K. Chouhan, A. Thayer, Y. Mudryk, I. Z. Hlova, O. Dolotko, and V. K. Pecharsky, “Unusual first-order magnetic phase transition and large magnetocaloric effect in Nd_2In ”, *Physical Review Materials* **6**, 114406 (2022)

-
- ⁴⁰ W. Liu, F. Scheibel, T. Gottschall, E. Bykov, I. Dirba, K. Skokov, and O. Gutfleisch, “Large magnetic entropy change in Nd₂In near the boiling temperature of natural gas”, *Applied Physics Letters* **119**, 022408 (2021).
- ⁴¹ W. Cui, G. Yao, S. sun, Q. Wang, J. Zhu, and S. Yang, “Unconventional metamagnetic phase transition in R₂In (R=Nd, Pr) with lamda-like specific heat and nonhysteresis”, *Journal of Materials Science & Technology* **101**, 80 (2022).
- ⁴² O. Gutfleisch, T. Gottschall, M. Fries, D. Benke, I. Radulov, K. P. Skokov, H. Wende, M. Gruner, M. Acet, P. Entel, and M. Farle, “Mastering hysteresis in magnetocaloric materials”, *Philosophical Transactions A* **374**, 20150308 (2016).
- ⁴³ A. Biswas, Y. Mudryk, A. K. Pathak, L. Zhou, and V. K. Pecharsky, “Managing hysteresis of Gd₅Si₂Ge₂ by magnetic field cycling”, *Journal of Applied Physics* **126**, 243902 (2019).
- ⁴⁴ F. X. Hu, B. Shen, J. Sun, and Z. Cheng, “Influence of negative lattice expansion and metamagnetic transition on magnetic entropy change in the compound LaFe_{11.4}Si_{1.6}”, *Applied Physics Letters* **78**, 3675 (2001).
- ⁴⁵ H. Zhang, Y. Sun, Y. Li, Y. Y. Yu, Y. Long, J. Shen, F. Hu, J. Sun, and B. G. Shen, “Mechanical properties and magnetocaloric effects in La(FeSi)₁₃ hydrides bonded with different epoxy resins”, *Journal of Applied Physics* **117**, 063902 (2015).
- ⁴⁶ Y. Mudryk, D. Paudyal, T. Prost, L.S. Chumbley, V.K. Pecharsky, and K.A. Gschneidner, Jr., “Correlations between magnetism, microstructure, crystallography, and phase stability in GdNi_{1-x}Co_x alloys”, *Acta Materialia* **92**, 18-24 (2015).
- ⁴⁷ M. Haldar, S. M. Yusuf, M. D. Mukadam, and K. Sashikala, “Magnetocaloric effect and critical behavior near the paramagnetic to ferrimagnetic phase transition temperature in TbCo_{2-x}Fe_x”, *Physical Review B* **81**, 174402 (2010).
- ⁴⁸ F. Guillou, H. Yibole, R. hamane, V. Hardy, Y. B. Sun, J. J. Zha0, Y. Mudryk, and V. K. Pecharsky, “Crystal structure and physical properties of Yb₂In and Eu_{2-x}Yb_xIn alloys”, *Physical Review Materials* **4**, 104402 (2020).

-
- ⁴⁹ E. Mendive-Tapia, D. Paudyal, L. Petit, and J. B. Staunton, “First-order ferromagnetic transitions of lanthanide local moments in divalent compounds: An itinerant electron positive feedback mechanism and Fermi surface topological change”, *Physical Review B* **101**, 174437 (2020).
- ⁵⁰ M. Forker, R. Mubeler, S. C. Bedi, M. Olzon-Dionysio, and S. Dionysio de Souza, “Magnetic and electric hyperfine interactions in the rare-earth indium compounds $R_2\text{In}$ studied by ^{111}Cd perturbed angular correlations”, *Physical Review B* **71**, 094404 (2005).
- ⁵¹ J. Rodriguez-Carvajal, “Recent advances in magnetic structure determination by neutron powder diffraction”, *Physica B* **192**, 55 (1993).
- ⁵² H. Naves Bez, H. Yibole, A. Pathak, Y. Mudryk, and V. K. Pecharsky, “Best practice in evaluation of the magnetocaloric effect from bulk magnetization measurements”, *Journal of Magnetism and Magnetic Materials*, 458, 301 (2018)
- ⁵³ P. G. de Gennes, D. saint-james, “Helical structures of the heavy rare earth metals”, *Solid State Communication* **1**, 62 (1963)
- ⁵⁴ S. A. law, S. L. Budko, P.C. Canfield, “Effects of mixed rare-earth occupancy on the low temperature properties of ($R, R', R'' \dots$) Ni_2Ge_2 single crystals”, *Journal of Magnetism and Magnetic Materials* **312**, 140 (2007)
- ⁵⁵ H. Gemari-Seale, T. Anagnostopoulos, and J. K. Yakinthos, “Magnetic characteristics of rare-earth indium $R_2\text{In}$ ($R = \text{Y, Nd, Sm, Gd, Dy, Ho, Er, and Tm}$) intermetallic compounds”, *Journal of Applied Physics* **50**, 434 (1979)
- ⁵⁶ J. Law, V. Franco, L. Moreno-Ramirez, A. Conde, D. Karpenkov, I. Radulov, K. P. Skokov, and O. Gutfleisch, “A quantitative criterion for determining the order of magnetic phase transitions using the magnetocaloric effect”, *Nature Communications* **9**, 2680 (2018).
- ⁵⁷ J. Cwik, T. Palewski, K. Nenkov, O. Gutfleisch, and J. Klamut, “The influence of Er substitution on magnetic and magnetocaloric properties of $\text{Dy}_{1-x}\text{Er}_x\text{Co}_2$ solid solutions”, *Intermetallics* **19**, 1656 (2011).

-
- ⁵⁸ Y. Mudryk, D. Paudyal, J. Liu, and V. K. Pecharsky, “Enhancing magnetic functionality with scandium: Breaking stereotypes in the design of rare earth materials”, *Chemistry of Materials* **29**, 3962 (2017).
- ⁵⁹ H. Zhang, B. G. Shen, Z. Y. Xu, J. Chen, J. Shen, F. X. Hu, and J. R. Sun, “Large reversible magnetocaloric effect in Er₂In compound”, *Journal of Alloys and Compounds* **509**, 2602 (2011).
- ⁶⁰ Q. Zhang, J. H. Cho, B. Li, W. J. Hu, and Z. D. Zhang, “Magnetocaloric effect in Ho₂In over a wide temperature range”, *Applied Physics Letters* **94**, 182501 (2009).
- ⁶¹ Q. Zhang, X. G. Liu, F. Yang, W. J. Feng, X. G. Zhao, D. J. Kang, and Z. D. Zhang, “Large reversible magnetocaloric effect in Dy₂In”, *Journal of Physics D: Applied Physics* **42**, 055011 (2009).
- ⁶² Y. S. Jia, T. Nakmiki, S. Kasai, L. W. Li, and K. Nishimura, “Magnetic anisotropy and large low field rotating magnetocaloric effect in NdGa single crystal”, *Journal of Alloys and Compounds* **757**, 44 (2018).
- ⁶³ L. Meng, Y. Jia, Y. Qi, Q. Wang, and L. Li, “Investigation of the magnetism and magnetocaloric effect in the R₂CoAl₃ (R = Gd, Tb, Dy and Ho) compounds”, *Journal of Alloys and Compounds* **715**, 242 (2017).
- ⁶⁴ C. M. Bonilla, J. Herro-Albillos, F. Bartolome, L. M. Garcia, M. Parra-Borderias, V. Franco, “Universal behavior for magnetic entropy change in magnetocaloric materials: An analysis on the nature of phase transitions”, *Physical Review B* **81**, 224424 (2010)
- ⁶⁵ J. Cwik, T. Palewski, K. Nenkov, O. Gutfleisch, and J. Klamut, “The influence of Er substitution on magnetic and magnetocaloric properties of Dy_{1-x}Er_xCo₂ solid solutions”, *Intermetallics* **19**, 1656 (2011).
- ⁶⁶ Y. Mudryk, D. Paudyal, J. Liu, and V. K. Pecharsky, “Enhancing magnetic functionality with scandium: Breaking stereotypes in the design of rare earth materials”, *Chemistry of Materials* **29**, 3962 (2017).

-
- ⁶⁷ H. Zhang, B. G. Shen, Z. Y. Xu, J. Chen, J. Shen, F. X. Hu, and J. R. Sun, “Large reversible magnetocaloric effect in Er₂In compound”, *Journal of Alloys and Compounds* **509**, 2602 (2011).
- ⁶⁸ Q. Zhang, J. H. Cho, B. Li, W. J. Hu, and Z. D. Zhang, “Magnetocaloric effect in Ho₂In over a wide temperature range”, *Applied Physics Letters* **94**, 182501 (2009).
- ⁶⁹ Q. Zhang, X. G. Liu, F. Yang, W. J. Feng, X. G. Zhao, D. J. Kang, and Z. D. Zhang, “Large reversible magnetocaloric effect in Dy₂In”, *Journal of Physics D: Applied Physics* **42**, 055011 (2009).
- ⁷⁰ Y. S. Jia, T. Nakmiki, S. Kasai, L. W. Li, and K. Nishimura, “Magnetic anisotropy and large low field rotating magnetocaloric effect in NdGa single crystal”, *Journal of Alloys and Compounds* **757**, 44 (2018).
- ⁷¹ L. Meng, Y. Jia, Y. Qi, Q. Wang, and L. Li, “Investigation of the magnetism and magnetocaloric effect in the R₂CoAl₃ (R = Gd, Tb, Dy and Ho) compounds”, *Journal of Alloys and Compounds* **715**, 242 (2017).
- ⁷² A. Biswas, S. Chandra, T. Samanta, B. Ghosh, S. Datta, M.H. Phan, A. K. Raychaudhuri, I. Das, H. Srikanth, “Universality in the entropy change for the inverse magnetocaloric effect”, *Physical Review B* **87**, 134420 (2013).
- ⁷³ A. Biswas, S. Chandra, T. Samanta, M. H. Phan, I. Das, and H. Srikanth, “The universal behavior of inverse magnetocaloric effect in antiferromagnetic materials”, *Journal of Applied Physics* **113**, 17A902 (2013)